SolarPACES 2024, 30th International Conference on Concentrating Solar Power, Thermal, and Chemical Energy Systems

Receivers and Heat Transfer Media and Transport: Linear Systems

https://doi.org/10.52825/solarpaces.v3i.2347

Published: 30 Jan. 2026

Numerical Investigation of Novel Parabolic Trough Receiver Configurations Using Liquid Sodium as Heat Transfer Fluid

Meriem Chaanaoui[1,*] and Justin Byiringiro[2,3]

[1]National School of Applied Sciences, Hassan First University, Berrechid 26100, Morocco

[2]Euromed University of Fes, UEMF, Fes, Morocco

[3]Rwanda Polytechnic, Kigali, Rwanda

*Correspondence: Meriem Chaanaoui, meriem.chaanaoui@uhp.ac.ma

Abstract. This paper conducts a numerical investigation of the performance improvement of a Parabolic Trough Collector (PTC) receiver using Computational Fluid Dynamics (CFD) simulations performed in ANSYS Fluent. The study aims to evaluate novel receiver configurations by comparing a conventional receiver (Case 1) with three innovative configurations (Cases 2, 3, and 4), using liquid sodium as the heat transfer fluid (HTF). The model's accuracy is validated against experimental data and theoretical expressions from the literature. Simulations are performed across various mass flow rates to assess key parameters, including the Nusselt number, friction coefficient, thermal efficiency, and circumferential temperature difference. The results indicate that Case 3 demonstrates the highest thermal performance among the configurations. Specifically, the novel receiver configurations consistently outperformed the conventional receiver. The Nusselt number increased by 29.84%, 126.1%, and 10%; the friction factor rose by 178%, 305%, and 17%; the thermal efficiency improved by 3.6%, 4%, and 3.4%; and the temperature difference decreased by 4.05%, 13.2%, and 1.31% for Confs 2, 3, and 4, respectively. Additionally, liquid sodium significantly enhanced the thermal performance of the PTC due to its superior thermal properties. These findings underscore the effectiveness of the proposed receiver configurations and the advantages of using liquid sodium as the HTF, offering a promising approach to improving PTC efficiency.

Keywords: Parabolic Trough Collector, Turbulator Inserts, Heat Transfer Enhancement, CFD

1. Introduction

Solar energy is a crucial strategy for addressing energy sector challenges, such as high greenhouse gas emissions from fossil fuels and rising global power consumption [1]. Common concentrated solar power (CSP) technologies include solar towers, solar dishes, linear Fresnel reflectors, and PTC [2]. Among these, PTCs are the most developed, extensively studied, and widely used in both hybrid and solar-only modes [3]. However, improving their heat transfer performance is essential to make PTC technology more competitive with conventional fossil energy sources. Previous studies have developed various techniques to improve the heat transfer of PTCs, generally categorized into passive and active methods [4],[5]. These improvements are achieved by increasing turbulence and delaying boundary layer formation, expanding the heat transfer area, or generating secondary rotating flows to enhance the heat transfer rate. Zou et al. [6] investigated a novel PTC receiver configuration to enhance heat

transfer, by using syltherm800 as HTF, and simulations were performed using CFD tool. It was noted that the highest increase in performance can be up to 30.1%. Chakrabortry et al. [7] investigated numerically the thermal performance of the LS-2 PTC model, where helical absorber tube was used with water as HTF. The observed enhancement in thermal efficiency was by 4% to 10%. Zhu et al. [8] studied the wavy-tape insert on the absorber tube of PTC using CFD simulation. The Nusselt number and friction factor were shown to improve by 3 and 4 times, respectively. Yilmaz et al. [9] used wire coil insert in the PTC receiver. Therminol VP1 was used as HTF, and numerical simulations were performed using ANSYS Fluent. It was observed that the heat transfer performance and thermal efficiency enhanced by 183 % and 1.4% respectively. Kursum [10] proposed a configuration of receiver tube of LS-2 PTC, by inserting internal longitudinal fins. Numerical simulations were conducted using ANSYS Fluent and Syltherm800 was used as HTF. Results showed the Nusselt number was enhanced between 25% to 78%. Recently studies using newly developed HTFs with improved thermophysical characteristics are reported in the literature for enhancing the convective heat transfer the PTC absorber tube. Bozorg et al. [11] used Al_2O_3/synthetic oil nanofluid in a PTC receiver containing porous structure and the thermal efficiency was observed to be increased by 8%. Kasaeian et al. [12] investigated experimentally a PTC receiver using MWCNT oil-based nanofluid as HTF. Efficiency was enhanced by 7% compared to oil HTF. Ali et al. [13] evaluated the PTC receiver performance enhancement. The receiver was equipped with a turbulator and Cuo-SWCNT/Water-based hybrid nanofluid was used as HTF. Thermal performance was observed to be improved by 3.85%. Krishna and kumar [14] assessed the use of liquid metals as HTF for PTC by exploring the heat transfer capabilities of various HTFs. They concluded that liquid sodium offers better enhancement of PTC performance compared to other examined HTFs. Kumar et al. [15] studied the thermal gradient and heat losses of the receiver for various collector aperture sizes and various HTFs, such as molten salt, liquid sodium, and NaK78. It was found that liquid sodium offers a significant reduction in temperature gradient as compared of other HTFs for all the aperture sizes of the collector, where the maximum reduction obtained is 85%.

From the above literature review it can be seen that combining turbulators and newly developed HTFs offers a unique opportunity to enhance PTC performance. Although several new HTFs have been developed, limited research has investigated the use of liquid metals in PTCs, particularly liquid sodium, which is widely used in the nuclear industry for its excellent thermal properties [16]. This study proposes innovative receiver configurations using liquid sodium as the HTF to enhance PTC thermal performance. The configurations are numerically analysed by coupling the finite volume method (FVM) with the Monte Carlo ray tracing (MCRT) method. The effects of mass flow rates and inlet velocity on parameters such as the Nusselt number, friction coefficient, thermal efficiency, and circumferential temperature difference are examined. This approach has the potential to increase power generation, improve heat production, and enhance thermal storage capacity, making PTC more competitive. The study is organized into five sections. Section two covers the materials and methods, section three defines the parameters, section four discusses the results, and section five presents the conclusion.

2. Material and methods

2.1 Geometrical modeling and HTF

This section presents three novel absorber tube configurations designed strategically modifying the conventional LS-2 PTC absorber (Figure 1.a). The modifications include the incorporation of internal obstacles, extending surfaces aimed at enhancing the thermal performance within the absorber. The conceptual development of these designs is grounded in established heat transfer enhancement techniques such as flow disruption, vortex generation, and increased surface area contact.

Case 2: Absorber with Y-shaped fin inserts

In this configuration (Figure 1.b), the internal fins are arranged in a Y-shape, creating diverging flow paths. These fins are strategically shaped to induce multiple recirculation zones and encourage complex secondary flow patterns. The splitting of flow caused by the Y-structure intensifies local turbulence and improves the interaction of fluid with the heated wall surface.

Case 3: Absorber with perforated fins and central rod

Figure 1.c presents a hybrid approach where perforated fins are combined with a central rod. The perforations in the fins function as micro-jets, injecting high-velocity streams into the flow field. These jets introduce additional momentum and actively disturb the thermal boundary layer, resulting in enhanced convective heat transfer. Simultaneously, the central rod enhances the flow disturbance in the core region, and the perforations also help reduce the pressure drop by allowing partial flow bypass through the fin openings.

Case 4: Absorber with Triangular Fins

The configuration in Figure 1.d employs triangular-shaped fins arranged longitudinally. The sharp edges of the triangular fins are designed to induce localised vortices as fluid flows past them. These vortices periodically disrupt the thermal boundary layer, facilitating better mixing and heat transfer. This configuration combines simplicity in fabrication with effective thermal performance gains. The fins act as vortex generators and are well-suited for retrofitting in existing absorber systems.

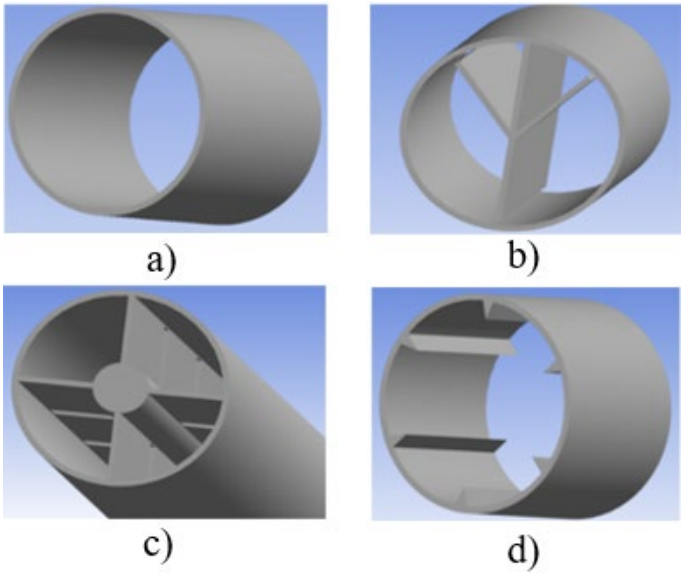

Figure 1. *Models of receivers: a) reference receiver (Case 1), b) Case 2, c) Case 3, d) Case 4*

The parameters and optical properties of the LS-2 receiver are listed in Table 1. The receiver tube and fins are made of 316L stainless, and the HTF used is Liquid sodium. The selection was based on our previous work [17], comparing it with Syltherm 800. That study showed that liquid sodium provides significantly better thermal performance due to its higher thermal conductivity and lower viscosity, which enhance heat transfer and reduce circumferential temperature gradients. However, its high chemical reactivity introduces notable safety and handling challenges. Thus, while liquid sodium offers clear receiver-level performance benefits, its use in large PTC fields must be balanced against these operational risks [17]. The thermo-physical properties of liquid sodium are presented in Table 2.

Table 1. *Characteristics of LS-2 PTC [18].*

Parameter	Value
Aperture width (m)	5
Focal length (m)	1.84
Module length (m)	7.8
Diameter of inner receiver (m)	0.066
Diameter of Outer receiver (m)	0.07
Absorptance	0.96
Reflectivity of the reflector	0.93

Table 2. *Thermo-physical properties of Liquid sodium [19].*

Property	Correlation
ρ (kg/m^3)	$\rho = 219 + 275.32\left(1 - \frac{T_f}{2503.7}\right) + 511.58\,(1 - \frac{T_f}{2503.7})^{0.5}$
Cp (J/kgK)	$1658.2 - 0.84790 \times T_f + 4.4541 \times 10^{-4} \times T^2 - 2.9926 \times 10^6 \times T_f^{-2}$
k (W/mK)	$124.67 - 0.11381 \times T_f + 5.5226 \times 10^{-5} \times T_f^{\,2} - 1.1842 \times 10^{-8} \times T_f^{\,3}$
$\ln(\mu)(\mathrm{kg/m.s})$	$-6.4406 - 0.3958\ln(T) + 556.835/T$

2.2 Numerical modeling

In this study, the Reynold averaged Navier-Stokes equations shown in Equations 1 to 3, are used to govern the heat transfer and fluid flow.

Continuity (1) momentum (2) and energy (3) equations;

$$\frac{\partial \rho}{\partial t} + \frac{\partial (\rho U_i)}{\partial x_i} = 0 \tag{1}$$

$$\frac{\partial \rho U}{\partial t} + \frac{\partial}{\partial x_j}\left(\mu\left(\frac{\partial U_i}{\partial x_j} + \frac{\partial U_j}{\partial x_i}\right) - \rho\overline{U'_\iota U'_J}\right) = -\frac{\partial p}{\partial x_i} \tag{2}$$

$$\frac{\partial \rho C_p T}{\partial t} + \frac{\partial}{\partial x_j}\left(\rho C_p U_j T\right) = -\lambda\frac{\partial T}{\partial x_j} \tag{3}$$

Where ρ is the fluid density (kg/m³), t is the time (s),U_i is the velocity component in the x_i direction (m/s), p is the pressure (Pa), μ is the dynamic viscosity (Pa·s), $\overline{U'_\iota U'_J}$ is the Reynolds stress tensor components (m²/s²), T is the temperature (K), C_p is the specific heat capacity at constant pressure (J/kg·K), and λ the thermal conductivity (W/m·K).

The governing equations are discretized and solved using, FVM and CFD implemented in ANSYS Fluent software. In this method, the computational domains of receivers are discretized into hexahedral elements. To perform the turbulence calculations, the Realizable k-epsilon model is used. To guarantee the convergence of the solution, the residual value for energy equation was less than 10^{-8}, while for other equations were less than 10^{-6}.

The boundary conditions were set as:

- Inlet: mass flow inlet, inlet temperature.
- Pressure outlet boundary condition with zero-gauge pressure.
- At the inner wall: A no-slip condition.
- No uniform heat flux on the receiver's exterior wall: The profile of heat flux is determined using the Monte Carlo Ray Tracing method.

The numerical model used in this study was validated using theoretical correlations from Gnielinski [20] and Petukhov [21], the model was also validated using Dudley's experiment [22]. The results for the numerical model were found to be in good agreement with correlation and experimental results. For more details information about the no-uniform heat flux modeling and the model validation, please refer to the author's previous study [23].

3. Parameters definitions

Parameters that will be used to evaluate the heat transfer performance of the PTC are defined in this section.

The Nusselt number is defined as,

$$Nu = \frac{h.D_H}{k} \tag{4}$$

Where, h, k and D_H are the heat transfer coefficient, the HTF thermal conductivity, and the hydraulic diameter respectively.

The heat transfer coefficient is given as,

$$h = \frac{Q_u}{(\pi.D_H.L).(T_r - T_{fm})} \tag{5}$$

where, Q_u, T_r and energy rate, receiver mean temperature, and HTF mean temperature respectively.

$$Q_u = m.c_p.(T_{out} - T_{in}) \tag{6}$$

Where, m, c_p, T_{out}, and T_{in} are HTF mass flow rate, HTF specific heat capacity, outlet temperature, and inlet temperature respectively.

The friction factor is defined as,

$$f = \frac{(\Delta P/l)\ .\ D_H}{\frac{1}{2}.\rho.V^2}. \tag{7}$$

Where, ΔP, ρ, V, and l are the pressure drop, density of HTF, inlet velocity, and length of the receiver, respectively.

$$Re = \frac{\rho.V.D_H}{\mu} \tag{8}$$

$$V = \frac{4m}{\rho.\pi.D_H^2} \tag{9}$$

The circumferential temperature difference is defined as,

$$\Delta T = T_{max} - T_{min} \tag{10}$$

Where T_{max} and T_{min} are the maximum and minimum temperatures around the receiver

4. Results and discussion

This study evaluated the heat transfer performance of different configurations by analyzing the Nusselt number, friction factor, and temperature distribution. This section presents the findings for each parameter.

4.1 Analysis of heat transfer.

The effect of altering the internal wall geometry of the receiver on heat transfer is shown in Figure 2. The heat transfer is evaluated using the Nusselt number, a dimensionless quantity representing the ratio of convective to conductive heat transfer across the boundary layer, calculated based on equation 4. An increase in flow rate leads to a higher Nusselt number, consistent with previous studies [6],[7],[10]. This occurs because, as the flow rate increases, the velocity of HTF through the receiver tube also rises. Higher velocity enhances turbulence, disrupting the thermal boundary layer. A thinner boundary layer improves convective heat transfer, resulting in a higher Nusselt number. The maximum increases in the Nusselt number are 29.847% for Case 2, 126.14% for Case 3, and 10.248% for Case 4. Configuration 3 outperformed other configurations. The fins create multiple channels for the flow, leading to intense mixing and a significant reduction in boundary layer thickness. The central core further constricts the flow, increasing velocity and turbulence. This results in the highest Nusselt number compared with other configurations (cases 2 and 4).

4.2 Analysis of flow resistance.

The resistance to flow due to friction is represented by the friction factor, calculated using Equation 8. Figure 3 shows the variation of the friction factor with mass flow rate. As the flow rate increases, the friction factor decreases. This behavior is attributed to the higher kinetic energy of the HTF, which reduces the influence of viscous forces and facilitates smoother flow. Increased flow rate results in thinner boundary layers along the receiver tube's inner surface, decreasing viscous drag and leading to reduced frictional losses. This finding aligns with fluid dynamics principles, where higher flow velocity reduces frictional resistance [10]. The maximum increase in friction factor is 160.73%, 249.3%, and 17.8%, for Cases 2, 3, and 4, respectively. Case 3 exhibits the highest friction factor, followed by Cases 2 and 4. This is due to its most obstructive and turbulence-inducing design, featuring a central core and multiple fins that increase surface area and create complex flow paths. The fluid encounters significant resistance as it navigates through this structure, leading to a higher friction factor. Case 2, with three fins extending from the inner wall of the tube, also generates turbulence and disrupts the flow, but to a lesser extent than Case 3. Compared to Syltherm800 used in the author's previous studies [22] for the conventional receiver (Case 1), Liquid-sodium shows reductions in friction factor by 66.72%, 475.09%, 86.55%, and 66.9% for Cases 1, 2, 3, and 4, respectively. This is because liquid sodium has a lower viscosity, which reduces resistance to flow. The decreased viscosity lessens energy losses from pressure drops, allowing smoother fluid movement within the system. Although the friction factor decreases at higher mass flow rates, the accompanying increase in flow velocity leads to a larger pressure drop according to Equation (8). Consequently, the pumping power requirement increases with mass flow rate, which must be considered when evaluating the overall thermal–hydraulic performance of the PTC.

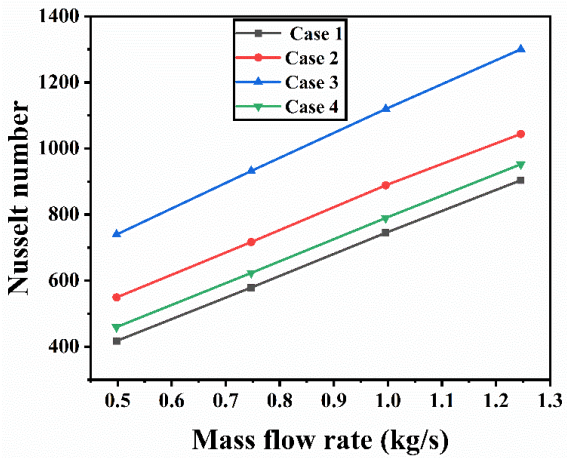

Figure 2. *Nusselt variation with mass flow rates*

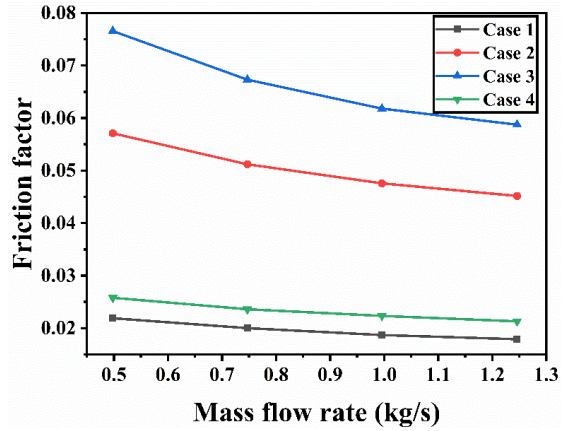

Figure 3. *Nusselt variation with mass flow rates*

4.3 Analysis of temperature distribution.

Figure 4 shows the HTF temperature distribution in the receiver cross-section at z = 3.8 m (middle of the receiver. At an inlet velocity of 0.6 m/s, the temperature difference (calculated based on Equation 10) is 38.5 K, 37 K, 34 K, and 38 K; at 1 m/s it is 29 K, 28 K, 25 K, and 28.4 K for cases 1, 2, 3, and 4 respectively. It is seen that the use of turbulators results in lower temperatures near the tube and a more uniform temperature distribution. Case 1 has an improper temperature distribution throughout the receiver's flow region, while the modified configurations (Cases 2, 3, and 4) produce better temperature distributions. This improvement is more pronounced at higher inlet velocities due to the turbulators creating rotational vortexes that enhance fluid flow mixing between the heated walls and the core flow zone. Furthermore, none of the configurations' temperature distributions are symmetrical about the tube's central axis due to the non-uniform heat flux on the receiver. From the discussion above it can be noted that increasing the heat transfer reduces the circumferential temperature difference of the absorber, which in turn reduces the thermal stresses on the receiver tube.

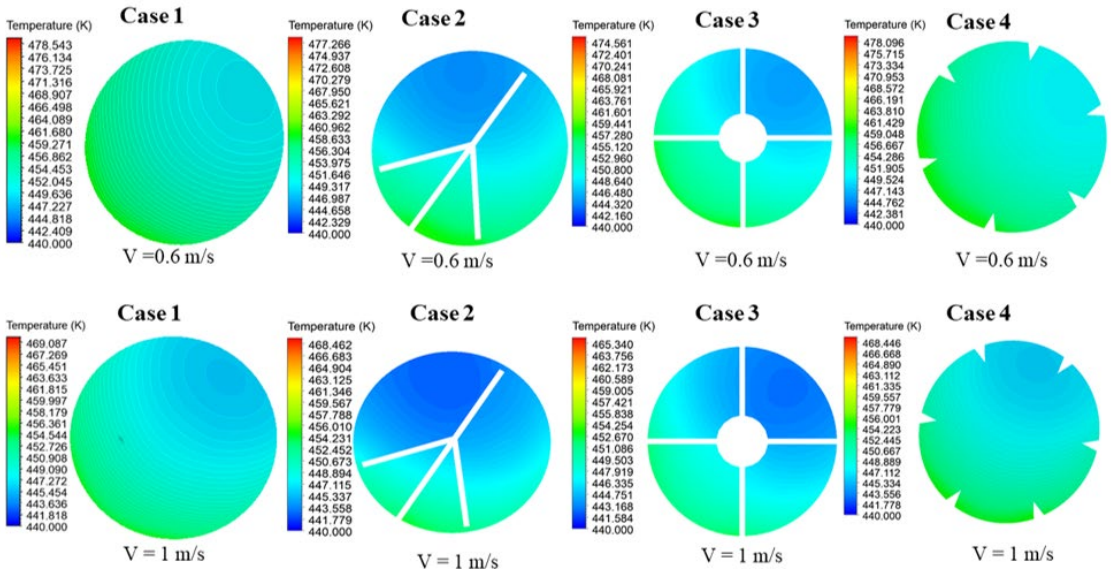

Figure 4. *Contours of temperature distribution through the absorber wall*

4.4 Summary of results

The performance improvements of cases 2, 3, and 4 compared to case 1 (the conventional receiver) are summarized in Table 2. Case 3 outperformed the other cases across all parameters, attributed to openings that allow more flow mixing.

Table 3. *Performance enhancement from different cases.*

Case	Nusselt number (%)	Friction factor (%)	Thermal efficiency (%)	Temperature difference (%)
Case 2	29.847	160.73	3.6	4.05
Case 3	126.14	249.3	4	13.2
Case 4	10.248	17.8	3.4	1.31

5. Conclusion

In this study, the heat transfer performance of PTC receivers was investigated numerically to evaluate new receiver configurations (Cases 2,3, and 4). The Nusselt number, friction factor, thermal efficiency, and temperature distribution for different mass flow rates were analyzed. The proposed configurations improved thermal efficiency and heat transfer, reducing the temperature difference and increasing the friction factor. The maximum increases in thermal efficiency, Nusselt number, friction factor, and reduction in temperature difference were 4%, 126.14%, 249.3%, and 13.2% respectively, for Case 3. Overall, the combination of innovative receiver configurations and liquid sodium shows great potential for enhancing the thermal performance of PTC receiver tubes.

Data availability statement

The data that support the findings of this study are available upon request to the corresponding author.

Author contributions

Meriem Chaanaoui: Writing – review & editing, Visualization, Validation, Software, Methodology, Investigation, Formal analysis, Supervision, Project administration,

Conceptualization, Resource. **Justin Byiringiro**: Writing – review & editing, Data curation, Visualization, Software, Methodology, Investigation, Conceptualization.

Competing interests

The authors declare that they have no competing interests.

References

[1] E. Bellos, C. Tzivanidis, D. Tsimpoukis, Enhancing the performance of parabolic trough collectors using nanofluids and turbulators, Renew. Sustain. Energy Rev. 91 (2018) 358–375. https://doi.org/10.1016/j.rser.2018.03.091.

[2] A. Bilal Awan, M.N. Khan, M. Zubair, E. Bellos, Commercial parabolic trough CSP plants: Research trends and technological advancements, Sol. Energy. 211 (2020) 1422–1458. https://doi.org/10.1016/j.solener.2020.09.072.

[3] A.M. Alaidaros, A.A. AlZahrani, Thermal performance of parabolic trough integrated with thermal energy storage using carbon dioxide, molten salt, and oil, J. Energy Storage. 78 (2024) 110084. https://doi.org/10.1016/j.est.2023.110084.

[4] Z.S. Kareem, M.N. Mohd Jaafar, T.M. Lazim, S. Abdullah, A.F. Abdulwahid, Passive heat transfer enhancement review in corrugation, Exp. Therm. Fluid Sci. 68 (2015) 22–38. https://doi.org/10.1016/j.expthermflusci.2015.04.012.

[5] J. Byiringiro, M. Chaanaoui, M. Halimi, S. Vaudreuil, Heat transfer improvement using additive manufacturing technologies: a review, Arch. Mater. Sci. Eng. 123 (2023) 30–41. https://doi.org/10.5604/01.3001.0053.9781.

[6] B. Zou, Y. Jiang, Y. Yao, H. Yang, Thermal performance improvement using unilateral spiral ribbed absorber tube for parabolic trough solar collector, Sol. Energy. 183 (2019) 371–385. https://doi.org/10.1016/j.solener.2019.03.048.

[7] O. Chakraborty, S. Roy, B. Das, R. Gupta, Effects of helical absorber tube on the energy and exergy analysis of parabolic solar trough collector – A computational analysis, Sustain. Energy Technol. Assessments. 44 (2021) 101083. https://doi.org/10.1016/j.seta.2021.101083.

[8] X. Zhu, L. Zhu, J. Zhao, Wavy-tape insert designed for managing highly concentrated solar energy on absorber tube of parabolic trough receiver, Energy. 141 (2017) 1146–1155. https://doi.org/10.1016/j.energy.2017.10.010.

[9] İ.H. Yılmaz, A. Mwesigye, T.T. Göksu, Enhancing the overall thermal performance of a large aperture parabolic trough solar collector using wire coil inserts, Sustain. Energy Technol. Assessments. 39 (2020). https://doi.org/10.1016/j.seta.2020.100696.

[10] B. Kurşun, Thermal performance assessment of internal longitudinal fins with sinusoidal lateral surfaces in parabolic trough receiver tubes, Renew. Energy. 140 (2019) 816–827. https://doi.org/10.1016/j.renene.2019.03.106.

[11] M.V. Bozorg, M. Hossein Doranehgard, K. Hong, Q. Xiong, CFD study of heat transfer and fluid flow in a parabolic trough solar receiver with internal annular porous structure and synthetic oil–Al2O3 nanofluid, Renew. Energy. 145 (2020) 2598–2614. https://doi.org/10.1016/j.renene.2019.08.042.

[12] A. Kasaeian, S. Daviran, R.D. Azarian, A. Rashidi, Performance evaluation and nanofluid using capability study of a solar parabolic trough collector, Energy Convers. Manag. 89 (2015) 368–375. https://doi.org/10.1016/j.enconman.2014.09.056.

[13] A. Hosseini esfahani, M. Aliehyaei, A.H. Joshaghani, M.M. Najafizadeh, Energy, exergy, economic and environmental analysis of parabolic trough collector containing hybrid nanofluid equipped with turbulator, Eng. Anal. Bound. Elem. 150 (2023) 492–506. https://doi.org/10.1016/j.enganabound.2023.02.031.

[14] N.V.V. Krishna Chaitanya, K. Ravi Kumar, Assessment of liquid metals as heat transfer fluid for parabolic trough solar collector, ISES Sol. World Congr. 2017 - IEA SHC Int. Conf. Sol. Heat. Cool. Build. Ind. 2017, Proc. (2017) 97–108. https://doi.org/10.18086/swc.2017.04.06.

[15] D. Kumar, K. Ravi, S.C. Kaushik, Heat transfer analysis of receiver for large aperture

parabolic trough solar collector, (2019) 1–17. https://doi.org/10.1002/er.4554.
[16] A. Mwesigye, İ.H. Yılmaz, Thermal and thermodynamic benchmarking of liquid heat transfer fluids in a high concentration ratio parabolic trough solar collector system, J. Mol. Liq. 319 (2020). https://doi.org/10.1016/j.molliq.2020.114151.
[17] Byiringiro, J., Chaanaoui, M., & Hammouti, B. (2025). Enhancement of thermal performance in parabolic trough solar Collectors: Investigation of three novel receiver configurations using advanced heat transfer fluids. Solar Energy Materials and Solar Cells, 293, 113833.
[18] K. Arshad Ahmed, E. Natarajan, Thermal performance enhancement in a parabolic trough receiver tube with internal toroidal rings: A numerical investigation, Appl. Therm. Eng. 162 (2019) 114224. https://doi.org/10.1016/j.applthermaleng.2019.114224.
[19] J. Liu, Y. He, X. Lei, Heat-transfer characteristics of liquid sodium in a solar receiver tube with a nonuniform heat flux, Energies. 12 (2019). https://doi.org/10.3390/en12081432.
[20] Ammar SM, Park CW. Validation of the Gnielinski correlation for evaluation of heat transfer coefficient of enhanced tubes by non-linear regression model: An experimental study of absorption refrigeration system. Int Commun Heat Mass Transf 2020;118:104819. https://doi.org/10.1016/j.icheatmasstransfer.2020.104819.
[21] Petukhov BS. Heat Transfer and Friction in Turbulent Pipe Flow with Variable Physical Properties. Adv Heat Transf 1970;6:503–64. https://doi.org/10.1016/S0065-2717(08)70153-9.
[22] E. Dudley, J. Kolb, A. Mahoney, T. Mancini, S. M, D. Kearney, Test results: SEGS LS-2 solar collector. Sandia National Laboratory. Report: SAND94- 1884, (1994) 140.
[23] J. Byiringiro, M. Chaanaoui, M. Halimi, Heat transfer enhancement of a parabolic trough solar collector using innovative receiver configurations combined with a hybrid nanofluid : CFD analysis, Renew. Energy. 233 (2024) 121169. https://doi.org/10.1016/j.renene.2024.121169.